Available online at www.sciencedirect.com
ScienceDirect
Trans. Nonferrous Met. Soc. China 32(2022) 2428−2437
Transactions of Nonferrous Metals Society of China
www.tnmsc.cn

Direct oxygen removal from titanium aluminide scraps by yttrium reduction

Li-na JIAO[1,2], Qi-sheng FENG[1], Shi-yu HE[1], Bao-hua DUAN[1], Zhi-he DOU[3], Chong-he LI[1,4], Xiong-gang LU[1,4,5]

1. State Key Laboratory of Advanced Special Steel & Shanghai Key Laboratory of Advanced Ferrometallurgy & School of Materials Science and Engineering, Shanghai University, Shanghai 200072, China;
2. School of Metallurgy and Materials Engineering, Jiangsu University of Science and Technology, Zhangjiagang 215600, China;
3. Key Laboratory for Ecological Metallurgy of Multimetallic Mineral, Ministry of Education, Northeastern University, Shenyang 110819, China;
4. Shanghai Special Casting Engineering Technology Research Center, Shanghai 201605, China;
5. School of Materials Science and Engineering, Shanghai Dianji University, Shanghai 201306, China

Received 21 April 2021; accepted 31 December 2021

Abstract: Titanium aluminum (TiAl) scraps with a high oxygen content were treated with yttrium (Y) in a liquid chemical deoxidization process for recycling. The Gibbs free energy and the equilibrium constant of the deoxidization reaction were calculated, and the effects of the yttrium content and the system pressure on the oxygen content in the product were determined. The results showed that the oxygen in TiAl scraps could be removed by yttrium, and the oxygen content of the deoxidized TiAl scraps had only 10% of the original content after deoxidization. Furthermore, the oxygen content of the deoxidized TiAl scraps was decreased with the increase of yttrium addition. The higher the chamber pressure, the greater the oxygen content in the final TiAl alloys. These results were consistent with calculated values. The microstructure of the deoxidized alloys was akin to that of the original material; however, Y_2O_3 particles were observed in the deoxidized alloys.

Key words: titanium aluminum scrap; yttrium; deoxidation; recycling

1 Introduction

Titanium aluminum (TiAl) alloys have been widely applied in the automobile and aerospace industries due to their light weight, high specific strength, high temperature resistance, high corrosion resistance, and excellent oxidation resistance [1−3]; however, they incur higher costs than other structural materials owing to their high temperature reactivity [4]. The preparation of TiAl alloys is difficult due to their strong affinity for oxygen. The recycling and reuse of material scraps can reduce the production cost, but the oxygen content in TiAl scraps is usually much higher than that in sponge titanium [5]. The oxygen content in TiAl alloys changes many of their properties [6,7], therefore, scraps with a relatively high oxygen content cannot be reused directly as the raw material for TiAl alloy production [8]. In order to use TiAl scraps as raw material, the oxygen dissolved in the scraps must be firstly removed. However, the oxygen which can be dissolved in titanium, is difficult to be removed from titanium alloys [9].

As demand for TiAl alloys is increasing in

Corresponding author: Chong-he LI, Tel: +86-13501773062, E-mail: chli@staff.shu.edu.cn;
Xiong-gang LU, Tel: +86-21-20685177, E-mail: luxg@shu.edu.cn
DOI: 10.1016/S1003-6326(22)65958-2

various industries (especially in the aerospace industry), deoxidation methods for TiAl scraps have become increasingly important in recent years [10]. Many techniques have been developed and investigated to remove oxygen directly from Ti and its alloys. In the process of calcium-halide flux deoxidation, the oxygen content of titanium can be reduced to 0.05 wt.% by reducing the activity of the deoxidation reaction product (CaO) in the $CaCl_2$ flux [11,12]. CHEN et al [13,14] applied the electrochemical deoxidation method to reduce TiO_2 directly. This process was named the FFC (Fray-Farthing-Chen) Cambridge method. Under equilibrium conditions with Ca and $CaCl_2$, the deoxidation of titanium dioxide has been explored elsewhere [15]. ZHENG et al [16] found that titanium with 0.02 wt.% of oxygen can be obtained under the Y/YOCl/YCl_3 equilibrium at 1300 K (1027 °C); however, due to the low process efficiencies enshrined in the methods, none of these electrochemical deoxidation approaches have worked outside the laboratory to date. MIMURA et al [17] proved that hydrogen can reduce the oxygen content in titanium, and this method was named hydrogenation and dehydrogenation (HDH), but it is difficult to remove all of the hydrogen in the HDH process.

Recently, an effective technique for preparing pure Ti and TiAl alloys by inducing melting processes using Ca as a deoxidizer has been developed [18]. In this process, the main principle of controlling the oxygen content of titanium is to introduce calcium to the molten metal or slag as a deoxidant [19]; however, the stability of CaO was found to be lower than that of Ti−0.2wt.%O at temperatures above 1600 K [20]. Therefore, Ca cannot reduce the oxygen content of Ti−O solid solutions to less than 0.2 wt.% at temperatures above 1600 K.

In recent years, the removal of O using rare-earth metals as deoxidants in the electrochemical deoxidation technique of Ti has been studied [21−24]. The oxygen content in Ti can be decreased to below 0.1 wt.% under Mg/$MgCl_2$/$HoCl_3$/HoOCl equilibrium by using the electrochemical method [21,22]. Oxygen content in Ti is decreased to less than 0.02 wt.% under Ho/HoOCl/$HoCl_3$ equilibrium, and the deoxidation of Ti by Ho in a $HoCl_3$ flux is effective [23]. When Y is used as a deoxidizer in a YCl_3 flux, the content of oxygen in Ti can be decreased to below 0.1 wt.% [24]. According to the Gibbs free energy, Y_2O_3 is stabler than CaO. The oxygen potentials of oxides for the formation of TiO_2, TiO, CaO, and Y_2O_3 are shown in Fig. 1 (as obtained from HSC software). Therefore, yttrium is a more efficient deoxidizing agent than calcium. However, the yttrium and oxygen deoxidation behavior in molten TiAl alloys has not yet been investigated. The present study focuses on recycling TiAl scraps via the vacuum induction melting process coupled with yttrium treatment.

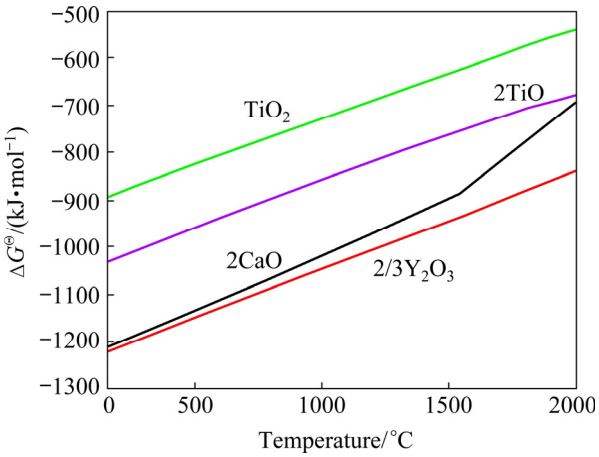

Fig. 1 Comparison of oxygen partial potentials of oxide in Ellingham diagram

2 Experimental

A schematic of the experimental apparatus is illustrated in Fig. 2. The vacuum electromagnetic levitation melting furnace consists of a water-cooled copper crucible and a vacuum chamber. The scraps of Ti−46Al−8Nb alloy, metallic yttrium and calcium fluoride slag were melted in the crucible, and the deoxidation reaction was performed in a high-purity argon atmosphere. At the slag−metal interface, oxygen in TiAl reacted with Y to realize deoxidation, and the deoxidation product Y_2O_3 was

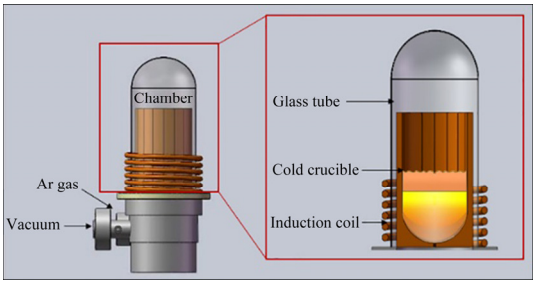

Fig. 2 Schematic of experimental apparatus

absorbed in the CaF_2. Several process parameters could affect the deoxygenation process, including the argon pressure, reaction temperature, reaction time, and added amount of Y. In the present study, the influence of the chamber pressure of argon and the amount of yttrium addition were evaluated.

The targeted composition for each melt was Ti−46Al−8Nb (at.%). The oxygen content in raw alloys was adjusted by adding titanium dioxide. The oxygen content of the raw TiAl alloys was analyzed. It was found that there were two groups of oxygen content, 0.62−0.65 wt.% and 0.81−0.87 wt.%, respectively. The equilibrium equation of oxygen and yttrium dissolved in the TiAl melt is described as follows:

$$2Y+3O=Y_2O_3(s) \quad (1)$$

To determine the amount of deoxidizer Y, the theoretical addition of deoxidizer Y was determined by Eq. (1). To estimate the effect of excessive Y on deoxidation, deoxidation experiments were conducted on five patterns of Y at 1.1, 1.3, 1.5, 1.7 and 1.9 times the base amount, and the five samples were defined as 1#−5#, respectively.

To avoid the reaction of TiAl alloys with oxygen gas in the air, the vessel was evacuated to 0.1×10^5 Pa and then filled with high-purity argon (99.99 vol.%) to the desired process pressure. The temperature was measured through the silica glass by using infrared radiation thermometers. When the liquidus temperature was reached, the CaF_2 slag bath sank through the molten metal bath, while the solid Y_2O_3 and non-metallic inclusions would be absorbed into the slag. The process should last long enough to let the molten alloys settle and separate from the resulting slag system. The metal solidified in the water-cooled copper crucible after the power supply was turned off. Below the molten metal, a thin slag skin with a thickness of 1 to 2 mm was formed. It reduced the heat loss and thus the cooling rate of ingot. Thus, the molten metal bath was protected from direct contact with the copper surface, which prevented the rate of solidification from being too fast and the uneven process, thus resulting in a high-quality finished surface [25].

After the deoxidation melting process, the ingot was removed from the crucible. The slag specimens were taken for further analysis. The button of ingot was re-melted three times to minimize segregation and ensure its homogeneity. Three parallel deoxidation trials were carried out in which TiAl scraps were made of the same components to ensure consistency. Since volatile elements (Ca and F) were still present after vacuum induction melting, an additional refining step was adopted.

Metal specimens were taken by electric spark cutting from the ingots at five different locations along the ingot centerline, which allowed the distinction between composition in the ingot center and the surface. The morphology of the deoxidized alloys was determined by scanning electron microscopy (SEM), and the distribution of different elements was analyzed by energy-dispersive X-ray spectrometry (EDS). Oxygen content was investigated using a LECO ONH836 analyzer. The dissolution content of element Y was obtained by using inductively coupled plasma optical emission spectrometer (ICP-OES) method. Five specimens were assayed and the average value was calculated.

3 Results and discussion

3.1 Removability of oxygen

According to the GB/T 3620.1—2007 standard [26], the oxygen content in most TiAl- based alloys should be less than 0.15 wt.%. To determine the deoxidation effect of TiAl alloys at different yttrium contents, the effect of the yttrium content was determined, as shown in Fig. 3 (red line). The oxygen content of the raw TiAl alloys was analyzed and found to be approximately 0.6 wt.%. With increasing addition of Y, the change in the oxygen content of these ingots decreased, especially when 1.9 times the base amount of Y was added,

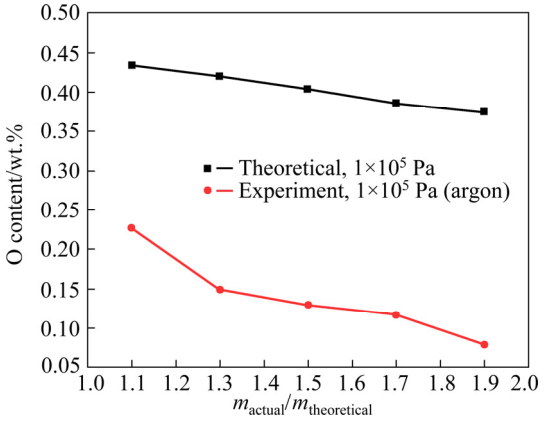

Fig. 3 Relationship between O content and Y content in deoxidized TiAl alloys at 1973 K (m_{actual} and $m_{theoretical}$ are actual and theoretical contents of Y, respectively)

the oxygen content of the ingot after yttrium treatment was 0.08 wt.%, which was far lower than the permitted maximum oxygen content [26]. The oxygen content of TiAl alloys after deoxidation suggests that the new technique exhibited an excellent deoxidation effect; however, when 1.1 times the base amount of Y was added, the oxygen content of ingots was 0.227 wt.%. In that case, insufficient deoxidizer Y was present in the molten TiAl, which led to insufficient deoxidation during the melting process.

Thermodynamic calculations were used to measure the content of yttrium for deoxidation of TiAl alloys. The equilibrium of oxygen in TiAl equilibrated with Y is described by

$$\mathrm{TiAl[O}_a\mathrm{](l)}+b\mathrm{Y(l)=TiAl[O}_m\mathrm{](l)}+b/2\mathrm{Y_2O_3(s)} \quad (2)$$

As yttrium has extremely low solubility in TiAl solution, the influence of the dissolution of yttrium on the Gibbs free energy of the system is ignored, and the Gibbs free energy of TiAl is approximately linear when the change in oxygen content is small. The Gibbs free energy of deoxygenation of Reaction (2) is calculated as follows:

$$\Delta G^{\Theta}=(1-3/2b)G_{\mathrm{f}}(\mathrm{TiAl[O}_m\mathrm{]})+b/2G_{\mathrm{f}}(\mathrm{Y_2O_3})-bG_{\mathrm{f}}(\mathrm{Y})-G_{\mathrm{f}}(\mathrm{TiAl[O}_a\mathrm{]}) \quad (3)$$

where a and b represent the molar amount of oxygen and yttrium in the TiAl melt, respectively; m is the molar amount of oxygen after deoxidation; $G_{\mathrm{f}}(\mathrm{TiAl[O}_a\mathrm{]})$ and $G_{\mathrm{f}}(\mathrm{TiAl[O}_m\mathrm{]})$ are the Gibbs free energy of TiAl alloys with the dissolved oxygen, respectively; $G_{\mathrm{f}}(\mathrm{Y_2O_3})$ and $G_{\mathrm{f}}(\mathrm{Y})$ denote the Gibbs free energy of formation of Y_2O_3 and Y, respectively.

At 1973 K and under the standard atmospheric pressure, the Gibbs free energy of oxygen dissolution in TiAl alloys melt can be determined by the Ti−Al−O ternary phase diagram as evaluated by QIU et al [27]. The oxygen content of the raw TiAl alloys is 0.6 wt.%, and the result from Eq. (3) is displayed in Fig. 3 (black line). It can be seen that the change in the oxygen content of these ingots decreases with increasing addition of Y, which is agreement with the experimental results in the present study. The reason for the difference between the theoretical and experimental data is that the oxygen partial pressure during deoxidation melting is different from that used in Eq. (3).

KOBAYASHI and TSUKIHASHI [28] studied the relationship between residual yttrium and oxygen in TiAl alloys. The same method for theoretical calculation and derivation was used in the present study. The equilibrium constant of Reaction (1) is expressed by Eq. (4):

$$K=a_{\mathrm{Y_2O_3}}/[(f_{\mathrm{Y}}w_{\mathrm{Y}})^2(f_{\mathrm{O}}w_{\mathrm{O}})^3] \quad (4)$$

where K is the equilibrium constant of Reaction (1); $a_{\mathrm{Y_2O_3}}$ represents the activity of Y_2O_3 relative to pure solid Y_2O_3; f_{Y} and f_{O} are the activity coefficients of yttrium and oxygen in the pure liquid standard, respectively; w_{Y} and w_{O} are yttrium and oxygen contents of molten metal. Using the first-order interaction parameters, f_{Y} and f_{O} are expressed by Eqs. (5) and (6), respectively. The interaction parameters are given by Eq. (7):

$$\lg f_{\mathrm{Y}}=e_{\mathrm{Y}}^{\mathrm{Y}}w_{\mathrm{Y}}+e_{\mathrm{Y}}^{\mathrm{O}}w_{\mathrm{O}} \quad (5)$$

$$\lg f_{\mathrm{O}}=e_{\mathrm{O}}^{\mathrm{Y}}w_{\mathrm{Y}}+e_{\mathrm{O}}^{\mathrm{O}}w_{\mathrm{O}} \quad (6)$$

$$e_{\mathrm{O}}^{\mathrm{Y}}=e_{\mathrm{Y}}^{\mathrm{O}}M_{\mathrm{O}}/M_{\mathrm{Y}} \quad (7)$$

where $e_{\mathrm{Y}}^{\mathrm{Y}}$, $e_{\mathrm{Y}}^{\mathrm{O}}$, $e_{\mathrm{O}}^{\mathrm{Y}}$ and $e_{\mathrm{O}}^{\mathrm{O}}$ represent the interaction parameters, respectively. It is assumed that the self-interaction coefficients $e_{\mathrm{Y}}^{\mathrm{Y}}$ and $e_{\mathrm{O}}^{\mathrm{O}}$ can be ignored. Equation (4) can be rewritten as Eq. (8) using the thermodynamic relationships of Eqs. (5)−(7).

$$\lg(w_{\mathrm{Y}}^2w_{\mathrm{O}}^3)=\lg K-e_{\mathrm{Y}}^{\mathrm{O}}(2w_{\mathrm{O}}+3M_{\mathrm{O}}/M_{\mathrm{Y}}\cdot w_{\mathrm{Y}}) \quad (8)$$

KOBAYASHI and TSUKIHASHI [28] experimentally obtained values for the equilibrium constant of Reaction (1) ($\lg K$=−3.74) and the interaction parameter ($e_{\mathrm{Y}}^{\mathrm{O}}$=−0.508) at 1893 K [28]. Based on Eq. (8), the relationship between the concentrations of O and Y in molten TiAl is demonstrated in Fig. 4 (black line). This indicates that the content of O in TiAl decreases with increasing Y in the TiAl.

Figure 4 (red line) depicts the content variations of oxygen and yttrium in the TiAl deoxidized alloys after yttrium treatment. The oxygen content in TiAl deoxidized alloys (0.08 wt.%) was lower than the theoretical oxygen content in TiAl (0.139 wt.%). The reason for the difference between the theoretical and experimental data is that the reaction temperature is different from that used in Eq. [8] by KOBAYASHI and TSUKIHASHI [28]. This result matches the previous thermodynamic calculation results of the relationship between yttrium addition and oxygen content.

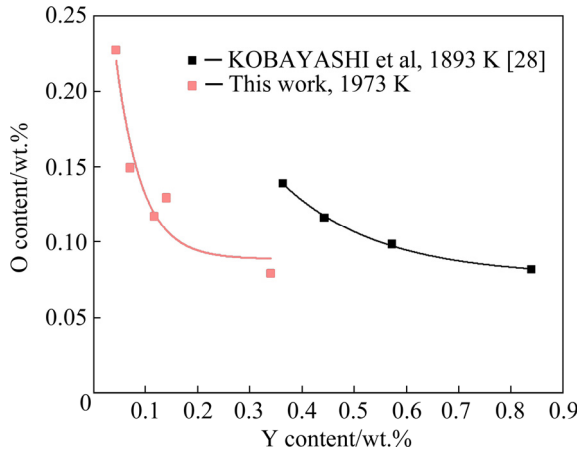

Fig. 4 Theoretical values of yttrium and saturated oxygen content in TiAl molten flux (black line) and experimental values of oxygen concentration in TiAl with change of yttrium content (red line)

To investigate the influence of the system pressure on the deoxidation effect, deoxidation experiments were performed by varying the system pressures in the range of 0.2×10^5 to 2.2×10^5 Pa. The oxygen content of the raw TiAl alloys was analyzed and found to be approximately 0.8 wt.%. The effects of changes in the oxygen content on the chamber pressure are illustrated in Fig. 5. With decreasing chamber pressure, the oxygen content in TiAl deoxidized ingots after yttrium treatment was reduced, especially when the chamber pressure was kept at 1×10^5 Pa, the oxygen content in the ingot after yttrium treatment was 0.129 wt.%. Thus, the lower chamber pressure improved the deoxidation efficiency of TiAl alloys for the conditions used in this study. The partial pressure of oxygen in the system decreased with the decrease of system pressure; however, as the system pressure was continually decreased, the oxygen content in the TiAl ingot after yttrium treatment was higher than that at the standard pressure (1×10^5 Pa). This was presumably because the refining process was more violent or even splashed in vacuum conditions, and the slag that sinks from the alloys to the bottom was involved in the melting of the alloy, which was not conducive to the removal of slag inclusions from TiAl alloys [29].

The dissolution reactions of gaseous oxygen into TiAl to form the solid solution and the Gibbs free energy change are expressed by Eqs. (9) and (10), respectively:

$$\frac{1}{2}O_2(g)=O\ (\text{in melt}) \tag{9}$$

$$\Delta G^{\Theta}_{\text{l,TiAl}}=-RT\ln(f_O w_O)/[(p_{O_2}/p^{\Theta})^{1/2}] \tag{10}$$

where $\Delta G^{\Theta}_{\text{l,TiAl}}$ represents the standard Gibbs energy change of oxygen dissolution in TiAl. The dissolution of oxygen in TiAl is expressed relative to the standard state of 1 wt.%. Considering that oxygen dissolved in TiAl obeys the Henry's law, the value of f_O is taken as 1.

According to Eq. (10), the oxygen content of TiAl is decreased with decreasing the partial pressure of oxygen, and the oxygen partial pressure is reduced by decreasing the system pressure. This is consistent with the experimental results in the present study.

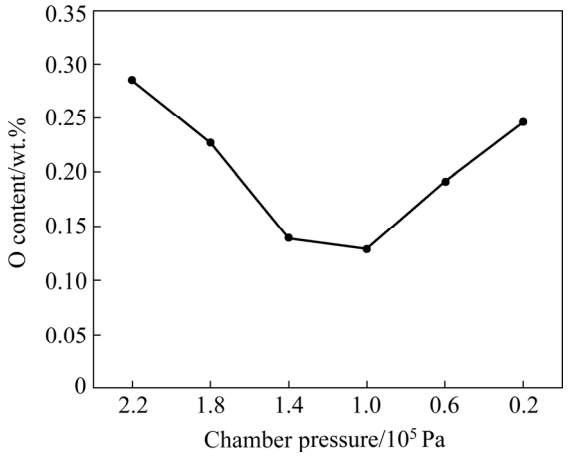

Fig. 5 Effect of chamber pressure on O content in TiAl deoxidized alloy

3.2 Characterization of deoxidation of TiAl alloys

To study the influence of yttrium treatment on the phase change of TiAl alloys, XRD was conducted on TiAl alloys after deoxidation, as shown in Fig. 6. The TiAl alloys (after deoxidation) consisted of two main phases (γ(TiAl) and α_2(Ti_3Al)), and no other phases were observed. IMAYEV et al [30] proved that TiAl and Ti_3Al phases were formed in the raw Ti−46Al−8Nb alloys. This result indicates that the phase structure of TiAl alloys does not change after deoxidation. Furthermore, the content of oxygen could not be identified because of the experimental accuracy of XRD. XRD patterns of the slags are shown in Fig. 7. The slag contained CaF_2 and Y_2O_3 phases, and no other phases were observed. This was because

yttrium reacted with dissolved oxygen in TiAl solution during the deoxidation process, which caused the formation of Y_2O_3 as a secondary phase.

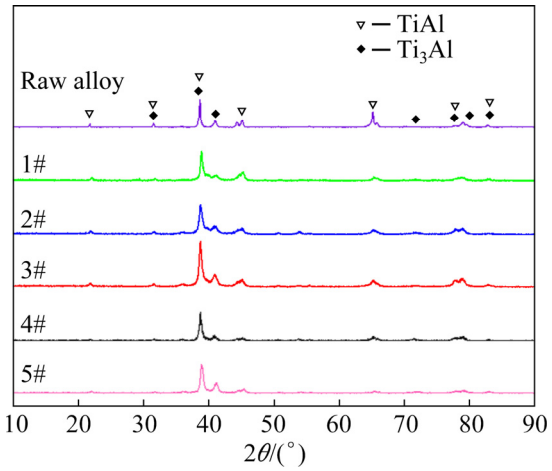

Fig. 6 XRD patterns of Ti−46Al−8Nb alloys after deoxidation

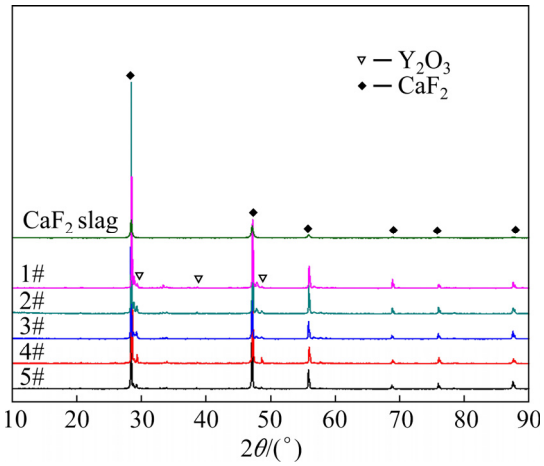

Fig. 7 XRD patterns of slags after deoxidation

The images of microstructure generated by secondary electrons of raw TiAl alloys and TiAl alloys after deoxidation are shown in Fig. 8. The results indicated that the microstructure of the specimens was quasi-lamellar, which consisted of two phases (α_2+γ), lamellar colonies, and a small blocky equiaxed γ phase. This phenomenon was also observed in XRD patterns (Fig. 6). These were typical microstructures of TiAl-based alloy, in which the Al content was slightly below 49 at.% [31]. There was no significant difference between the raw and deoxidized alloys, which implied that yttrium treatment had no effect on the microstructure of TiAl alloys after deoxidation.

To verify the feasibility of the deoxidation technology, the TiAl deoxidized alloys were also

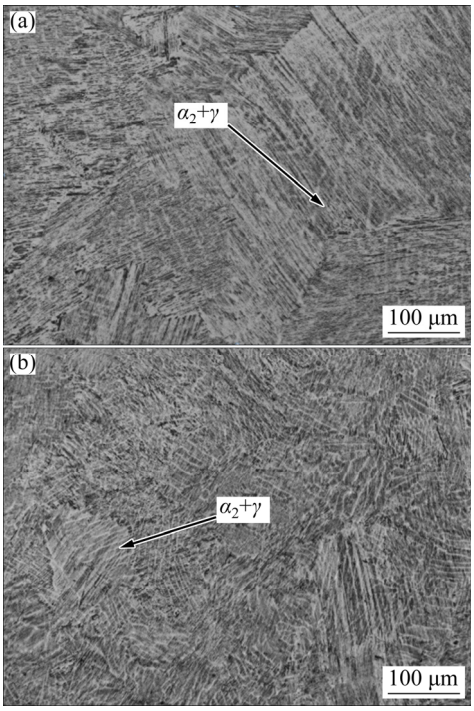

Fig. 8 Microstructures of raw Ti−46Al−8Nb alloy (a) and deoxidized Ti−46Al−8Nb alloy (b)

observed using SEM with the backscattered electron mode, which revealed the chemical contrast. The chemical composition of the phases was further identified by EDS. As shown in Fig. 9, according to the morphology of the alloy phase in the backscattered electron image, bright precipitates in the network were enriched at the grain boundary, and the inclusion phases embedded in TiAl matrix phase were in the form of white irregular blocks. The results of EDX analysis are displayed in Table 1. There was trace dissolved oxygen in the matrix phase. The molar ratio of Ti to Al to Nb was close to 46:46:8, which was consistent with that in Ti−46Al−8Nb alloy. The molar ratio of Y to O element was close to 2:3, which was in agreement with that in Y_2O_3, that is, the deoxidized product.

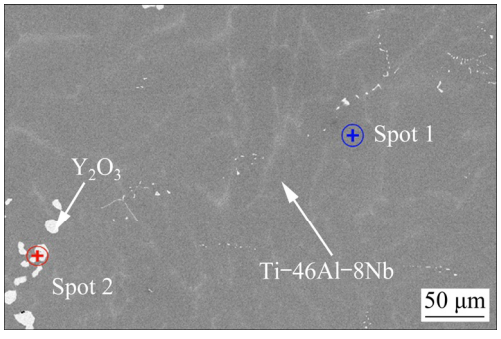

Fig. 9 Backscattered electron image of deoxidized alloy

Table 1 Chemical composition at Spot 1 and Spot 2 in Fig. 9

Spot No.	Content	O	Al	Y	Nb	Ti
1	wt.%	0.28	27.95	0.51	16.15	55.11
	at.%	0.73	43.45	0.24	7.29	48.29
2	wt.%	20.85	0	77.75	0	1.40
	at.%	59.04	0	39.63	0	1.33

3.3 Element distribution in TiAl alloys after deoxidation

The distribution of various elements in TiAl alloys after deoxidation is demonstrated in Fig. 10.

Figure 10 illustrates the SEM image and the corresponding EDX energy spectrum analysis of the alloy samples. The distribution and enrichment of five elements (Ti, Al, Nb, O, and Y) of the alloys were detected. In each image, the color depth of a certain area represents the density of elements in that area. Through the analysis of the individual elements of the elementary mapping, Ti, Al, and Nb in TiAl alloys after deoxidation were all distributed in the matrix phase, and oxygen was more concentrated at the positions where Y had been enriched, showing obvious negative segregation.

A line scan analysis of TiAl alloys after yttrium treatment was carried out to determine the concentration of different elements between the matrix phase and inclusion phase in deoxidized alloy. As shown in Fig. 11, the scanning line passed through the inclusion phase, and distributions of elements along the line were scanned on the backscattered electron image. According to the results of line scan spectrum analysis, a weak Y peak, along with O peak in the matrix phase, could be observed but the peak intensities of O and Y were enhanced in the inclusion phase. This finding suggested that O and Y were enriched in the inclusion phase. A strong Ti peak, along with Al and Nb peaks, could be observed in the matrix phase, but when scanning to the inclusion phase, the peak intensity of the three diminished. This result implied that O and Y were concentrated in the inclusion phase, and Ti, Al, and Nb were

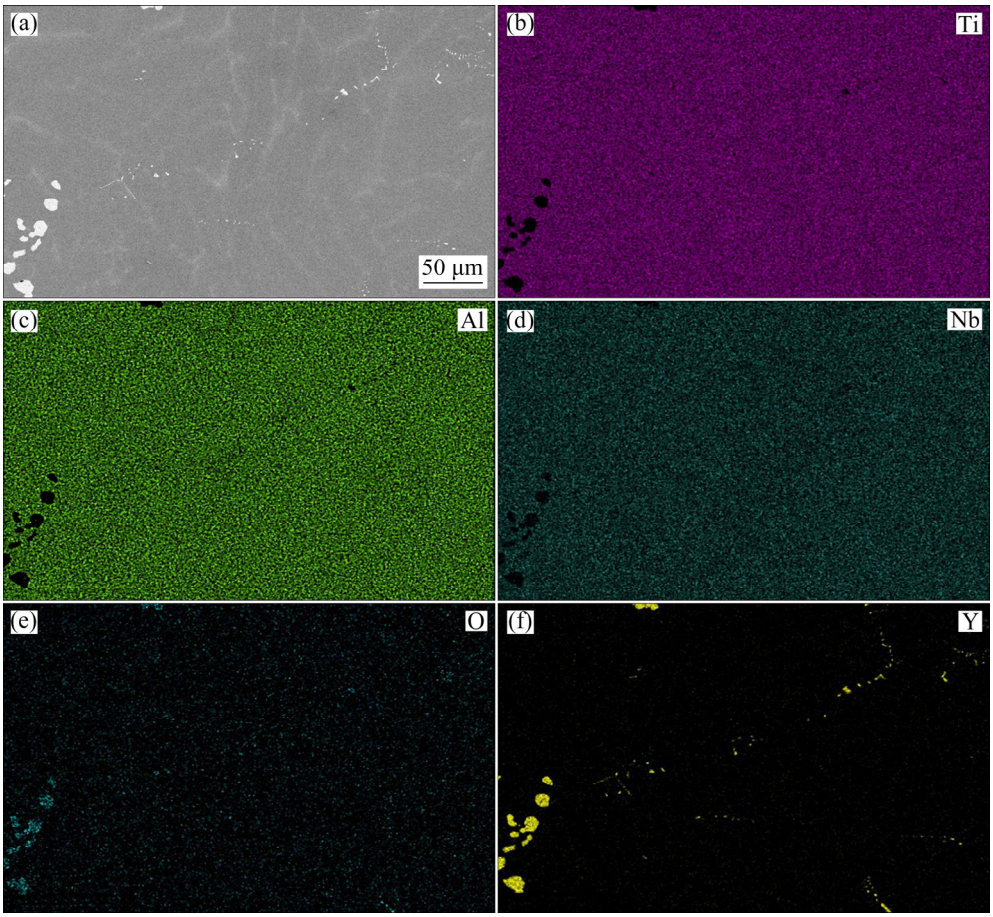

Fig. 10 Backscattered electron image of deoxidized alloy (a) and corresponding composition distribution maps (b−f) by EDX

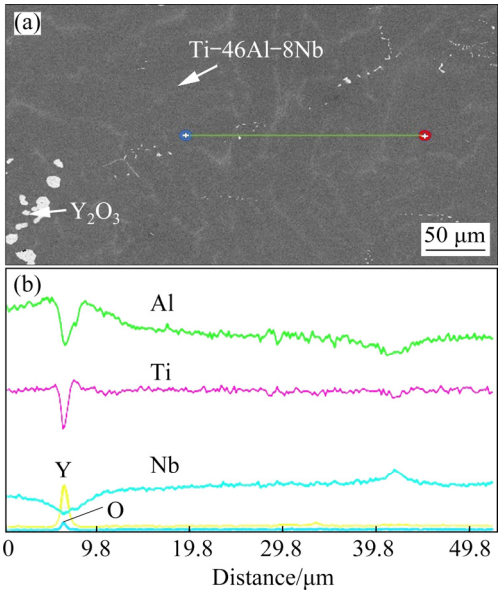

Fig. 11 Backscattered electron image (a) and line scan spectra (b) of deoxidized alloy

concentrated in the matrix phase. The same result was obtained in the element surface scanning spectrum in Fig. 10.

The utilization of the currently downgraded scrap fraction as feed material in a recycling process results in a new cost-competitive secondary titanium alloy. The interstitial O in the TiAl scraps was successfully reduced by the vacuum electromagnetic levitation melting process coupled with a yttrium treatment method, and the deoxidation effect was independent on the oxygen content in TiAl scraps, as described in our previous work [32]. Yttrium was found in the TiAl scraps after yttrium treatment. Analysis of microstructural and mechanical properties showed that a small amount of elemental Y formed Y_2O_3 particles which promoted nucleation, improved the plasticity, and enhanced the stiffness of the alloys [33−36]. This process can be applied to TiAl alloy, and further development is expected to achieve industrial feasibility.

4 Conclusions

(1) The oxygen in TiAl scraps could be removed by using the proposed method. The microstructure of deoxidized alloys was similar to that of the original scrap metal; however, Y_2O_3 particles were present in the matrix phase of the TiAl deoxidized alloys.

(2) Two methods for theoretical calculation and derivation of the Gibbs free energy change of deoxygenation reaction and the equilibrium constant of reaction were used. The results showed that the oxygen content in the alloys decreased with increasing yttrium content.

(3) The change of the oxygen content in TiAl alloys decreased with increase of Y, and these results were consistent with the calculated values.

(4) The change of the oxygen content in TiAl alloys decreased with decrease of system pressure. However, as the system pressure was continually decreased (to less than 1×10^5 Pa), the oxygen content in the TiAl ingot after yttrium treatment was higher than that under the standard pressure (1×10^5 Pa).

Acknowledgments

This work was supported by Key Laboratory for Ecological Metallurgy of Multimetallic Mineral (Ministry of Education) Open Subject, the National Natural Science Foundation of China — China Baowu Steel Group Joint Research Fund for Iron and Steel (No. U1860203), and the National Natural Science Foundation of China (No. U1760109).

References

[1] GÜTHER V, ALLEN M, KLOSE J, CLEMENS H. Metallurgical processing of titanium aluminides on industrial scale [J]. Intermetallics, 2018, 103: 12−22.

[2] LIU Zhan-qi, MA Rui-xin, XU Guo-jian, WANG Wen-bo, SU Yun-hai. Effects of annealing on microstructure and mechanical properties of γ-TiAl alloy fabricated via laser melting deposition [J]. Transactions of Nonferrous Metals Society of China, 2020, 30: 917−927.

[3] REN Li-rong, QIN Shui-jie, ZHAO Si-hao, XIAO Hua-qiang. Fabrication and mechanical properties of Ti_2AlC/TiAl composites with co-continuous network structure [J]. Transactions of Nonferrous Metals Society of China, 2021, 31: 2005−2012.

[4] OH J M, LEE B K, SUH C Y, CHO S W, LIM J W. Preparation method of Ti powder with oxygen concentration of <1000 ppm using Ca [J]. Powder Metallurgy, 2012, 55(5): 402−404.

[5] OKABE T H, HIROTA K, KASAI E, SAITO F, WASEDA Y, JACOB K T. Thermodynamic properties of oxygen in RE−O (RE=Gd, Tb, Dy, Er) solid solutions [J]. Journal of Alloys and Compounds, 1998, 279: 184−191.

[6] TAKEDA O, OKABE T H. Recycling of Ti [M]//Extractive Metallurgy of Titanium. Amsterdam: Elsevier Inc, 2020: 363−387.

[7] ZHAO Kun, OUYANG Si-hui, LIU Yong, LIU Bin, LIANG Xiao-peng, LI Hui-zhong, WANG Yu. Isothermal oxidation behavior of TiAl intermetallics with different oxygen

contents [J]. Transactions of Nonferrous Metals Society of China, 2019, 29: 526−533.

[8] CHEN Bo, MA Ying-che, GAO Ming, LIU Kui. Changes of oxygen content in molten TiAl alloys as a function of superheat during vacuum induction melting [J]. Journal of Materials Science & Technology, 2010, 26(10): 900−903.

[9] OKABE T H, JACOB K T T, WASEDA Y. The thermodynamics of oxygen in reactive metals [C]// Purification Process and Characterization of Ultra High Purity Metals. Berlin: Springer, 2002: 3−37.

[10] OKABE T H, OISHI T, ONO K. Deoxidation of titanium aluminide by Ca−Al alloy under controlled aluminum activity [J]. Metallurgical Transactions B, 1992, 23(5): 583−590.

[11] OKABE T H, OISHI T, ONO K. Preparation and characterization of extra-low-oxygen titanium [J]. Journal of Alloys and Compounds, 1992, 184: 43−56.

[12] SUZUKI R O, INOUE S. Calciothermic reduction of titanium oxide in molten $CaCl_2$ [J]. Metallurgical and Materials Transactions B, 2003, 34: 277−285.

[13] CHEN G Z, FRAY D J, FARTHING T W. Cathodic deoxygenation of the alpha case on titanium and alloys in molten calcium chloride [J]. Metallurgical and Materials Transactions B, 2001, 32: 1041−1052.

[14] CHEN G Z, FRAY D J, FARTHING T W. Direct electrochemical reduction of titanium dioxide to titanium in molten calcium chloride [J]. Nature, 2000, 407: 361−364.

[15] WANG Bin, LIU Kui-ren, CHEN Jian-she. Reaction mechanism of preparation of titanium by electro-deoxidation in molten salt [J]. Transactions of Nonferrous Metals Society of China, 2011, 21: 2327−2331.

[16] ZHENG Chen-yi, OUCHI T, IIZUKA A, TANINOUCHI Y K, OKABE T H. Deoxidation of titanium using Mg as deoxidant in $MgCl_2$−YCl_3 flux [J]. Metallurgical and Materials Transactions B, 2019, 50: 622−631.

[17] MIMURA K, KOMUKAI T, ISSHIKI M. Purification of chromium by hydrogen plasma-arc zone melting [J]. Materials Science and Engineering A, 2005, 403: 11−16.

[18] REITZ J, LOCHBICHLER C, FRIEDRICH B. Recycling of gamma titanium aluminide scrap from investment casting operations [J]. Intermetallics, 2011, 19: 762−768.

[19] TSUKIHASHI F, HATTA T, TAWARA E. Thermodynamics of calcium and oxygen in molten titanium and titanium−aluminum alloy [J]. Metallurgical and Materials Transactions B, 1996, 27: 967−972.

[20] MAH A D, KELLEY K K, GELLERT N L, KING E G, OBRIEN C J. Thermodynamic properties of titanium−oxygen solutions and compounds [M]. United States: Bureau of Mines, 1957.

[21] KONG L X, OUCHI T, ZHENG C Y, OKABE T H. Electrochemical deoxidation of titanium scrap in $MgCl_2$−$HoCl_3$ system [J]. Journal of the Electrochemical Society, 2019, 166(13): E429−E437.

[22] KONG Ling-xin, OUCHI T, OKABE T H. Direct deoxidation of Ti by Mg in $MgCl_2$−$HoCl_3$ flux [J]. Materials Transactions, 2019, 60(9): 2059−2068.

[23] KONG L X, OUCHI T, OKABE T H. Deoxidation of Ti using Ho in $HoCl_3$ flux and determination of thermodynamic data of HoOCl [J]. Journal of Alloys and Compounds, 2021, 863: 156047.

[24] IIZUKA A, OUCHI T, OKABE T H. Ultimate deoxidation method of titanium utilizing Y/YOCl/YCl_3 equilibrium [J]. Metallurgical and Materials Transactions B, 2020, 51(2): 433−442.

[25] FRIEDRICH B, BRINKMANN F, SCHWENK M. Generation of low oxygen Ti−Al−V-alloys from oxidic raw materials via aluminothermic reduction (ATR), subsequent refining via electroslag remelting (ESR) and vacuum arc remelting (VAR) [C]//3rd Ingot Casting, Rolling and Forging Conference (ICRF). Stockholm, Sweden, 2018.

[26] GB/T 3620.1—2007. Grades and chemical compositions of titanium and titanium alloys [S].

[27] QIU Ai-tao, LIU Lan-jie, PANG Wei, LU Xiong-gang, LI Chong-he. Calculation of phase diagram of Ti−Ni−O system and application to deoxidation of TiNi alloy [J]. Transactions of Nonferrous Metals Society of China, 2011, 21: 1808−1816.

[28] KOBAYASHI Y, TSUKIHASHI F. Thermodynamics of yttrium and oxygen in molten Ti, Ti_3Al, and TiAl [J]. Metallurgical and Materials Transactions B, 1998, 29: 1037−1042.

[29] LI Jun, WU En-hui, YANG Shao-li, HOU Jing, XU Zhong, HUANG Ping, MA Lan, JIANG Yan, LIU Qian-shu. Vacuum magnetic levitation refining for titanium aluminum alloy prepared by electro-thermal reduction [J]. Iron Steel Vanadium Titanium, 2019, 40(2): 41−49. (in Chinese)

[30] IMAYEV R M, IMAYEV V M, OEHRING M, APPEL F. Alloy design concepts for refined gamma titanium aluminide based alloys [J]. Intermetallics, 2007, 15: 451−460.

[31] XU X J, LIN J P, WANG Y L, GAO J F, LIN Z, CHEN G L. Microstructure and tensile properties of as-cast Ti−45Al−(8−9)Nb−(W, B, Y) alloy [J]. Journal of Alloys and Compounds, 2006, 414: 131−136.

[32] JIAO Li-na, WANG Shi-hua, XIONG F H, CHEN Guang-yao, DOU Zhi-he, LU Xiong-gang, LI Chong-he. Deoxidation of TiAl alloy scraps with metallic yttrium and calcium fluoride slag [C]//The Minerals, Metals & Materials Society (TMS). San Diego: Springer, 2020: 1691−1699.

[33] LIU Hai-yan, TANG Hui-ping, HE Wei-wei, LIU Yan-bin, JIA Wen-peng. Properties evolution of a powder metallurgical titanium alloy with yttrium addition [J]. Rare Metal Materials and Engineering, 2011, 40(S3): 298−300.

[34] ANINAT R, VALLE N, CHEMIN J B, DUDAY D, MICHOTTE C, PENOY M, BOURGEOIS L, CHOQUET P. Addition of Ta and Y in a hard Ti−Al−N PVD coating: Individual and conjugated effect on the oxidation and wear properties [J]. Corrosion Science, 2019, 156: 171−180.

[35] WU Y, HAGIHARA K, UMAKOSHI Y. Improvement of cyclic oxidation resistance of Y-containing TiAl-based alloys with equiaxial gamma microstructures [J]. Intermetallics, 2005, 13: 879−884.

[36] LI Qiang, YANG Zhi-dao, XIA Chao-qun, WANG Xing-hua, YANG Tai, LIANG Chun-yong, YIN Fu-xing, LIU Ri-ping. Effects of Y addition on microstructure and mechanical properties of Ti−25Zr alloys [J]. Materials Science and Engineering A, 2019, 748: 236−243.

钛铝合金废料钇还原法熔炼脱氧

焦丽娜[1,2]，冯齐胜[1]，何世宇[1]，段保华[1]，豆志河[3]，李重河[1,4]，鲁雄刚[1,4,5]

1. 上海大学 材料科学与工程学院，省部共建高品质特殊钢冶金与制备国家重点实验室，上海市钢铁冶金新技术开发应用重点实验室，上海 200072；
2. 江苏科技大学 冶金与材料工程学院，张家港 215600；
3. 东北大学 多金属共生矿生态化冶金教育部重点实验室，沈阳 110819；
4. 上海市特种铸造工程技术研究中心，上海 201605；
5. 上海电机学院 材料科学与工程学院, 上海 201306

摘 要：以钇为脱氧剂，采用熔炼脱氧工艺对高氧钛铝合金废料进行脱氧处理。计算脱氧反应的吉布斯自由能和平衡常数，考察钇含量和体系压力对 TiAl 脱氧合金氧含量的影响。结果表明，钇可以有效去除 TiAl 合金中的氧，脱氧后 TiAl 合金中的氧含量仅为原始合金废料中氧含量的 10%。此外，随着钇添加量的增加，TiAl 合金中氧含量降低；反应体系压力越高，TiAl 脱氧合金中的氧含量越高。这些结果与理论计算值一致。脱氧合金的显微组织与原始合金的相似，但在脱氧合金的基体相中观察到 Y_2O_3 夹杂物。

关键词：钛铝合金废料；钇；脱氧；回收利用

(Edited by Xiang-qun LI)